# Numerical and experimental fluid dynamics in the modern yacht design process

# NUMERICAL AND EXPERIMENTAL FLUID DYNAMICS IN THE MODERN YACHT DESIGN PROCESS

**IM Viola**, School of Marine Science and Technology, Newcastle University, UK
**S Bartesaghi**, Mechanical Engineering Department, Politecnico di Milano, Italy
**S Della Rosa,** Silverio Della Rosa Naval Architect, Milan, Italy
**S Cutolo,** Hydro Tec, Varazze, Italy

**SUMMARY**

There are three main methods to assess the hydrodynamic characteristics of yachts, namely, viscous and inviscid numerical analysis, and experimental tests. Computational tools are now widely used in yacht design because of the rapid growth of high-powered computers during the last 10 years. Viscous computational fluid dynamic codes are now one of the most important tools in design offices, in marine and other fields, and in some fields they have completely replaced inviscid codes and experimental tests. A deeper awareness of the uncertainty of RANS code results is necessary, achievable with a rigorous application of a verification and validation process.

The effectiveness of these three methods is discussed with regards to their application to yacht design of their hulls, hull appendages and propellers. The aim of this paper is to show that each of these three methods is very useful, having their own unique features, but the methods must be used with caution and a thorough understanding of their limitations, so as to provide a reliable suite of design tools.

## 1. INTRODUCTION

Two hundred years ago the design of vessels was mainly based on the experience of the designer and rarely on experimental measurements. In 1874, William Froude [1] recognised that the limitation of towing tank tests is the impossibility of modelling at the same time the full-scale ratio between inertial and viscous forces, namely the Reynolds number (*Re*), and the ratio between inertial and gravitational forces, namely the Froude number (*Fr*). It is common practice to scale the model in order to perform the test at the same *Fr* than in full scale. The measured total resistance is considered made of a component due to the wave generation, namely *wave resistance*, and a component due to the viscous effects, namely *viscous resistance*. It is also assumed that the wave resistance is mainly affected by *Fr*, while the viscous resistance is mainly affected by *Re*. Therefore the measured resistance is corrected a posteriori to take into account that the viscous resistance in full scale must be different from model scale being tested at a different *Re*. The studies by Prandtl [2] and by his students Von Karman [3] and Blasius [4], led to great insight on the boundary layer on flat plates. These studies allowed estimating the viscous resistance with several empirical formulations derived from measurements on flat plates. The curvature of the hull was then taken into account by further formulations developed in the 1950s [5, 6, 7]. It is interesting to note that these formulations are still in use today to correlate the model-scale resistance measured in the towing tank with the full-scale resistance.

In the 1970s, greatly improved computers allowed potential flow theory to be successfully applied in marine applications. This theory assumes the flow to be inviscid and irrotational, and allows modelling of non-dissipative flows. For instance, the lift generated by airfoils at angle of attack below the stall angle and the wave pattern generated by a vessel can be modelled with potential flow. Therefore, the wave resistance can be computed but the viscous resistance must be estimated with other methods.

The fluid dynamic equations, which take into account viscous effects, were developed in 1822 by Claude-Louis Navier [8] and then completed by Sir George Gabriel Stokes [9]. These equations, known as Navier-Stokes equations, are very difficult do be solved and only few analytical solutions are possible. For complex geometries, such as a hulls, a propellers, etc., the equations must be solved numerically (i.e. iterating through approximate solutions). The computational effort to solve them numerically depends on *Re*. At high *Re* the flow is turbulent and the turbulent fluctuations have a significant effect on the mean flow field. Therefore, the turbulent fluctuations must be taken into account in order to compute the mean flow field and, for instance, the resulting mean hull resistance. The largest turbulent structures are of the order of magnitude of the hull length *L*, and these break into smaller structures until dissipated by viscous effect. The higher the *Re*, the greater the difference between the smallest and the largest turbulent scales, and thus the higher the needed spatial resolution and the more expensive to solve the Navier-Stokes equations. Moreover, the smaller the turbulent structure then the shorter the oscillation of the velocity and pressure. Therefore, both the spatial and the time discretization should allow all the turbulent scales to be modelled. Such a simulation is very computationally demanding and it is called Direct Numerical Simulation (DNS). For instance, in 1988, Spalart [10] performed a milestone DNS of a turbulent flat-plate boundary layer up to $Re$=1400. Today, higher *Re* can be modeled but it is still impossible to perform DNS at the high *Re* values of interest to naval architects.

If the spatial and time resolutions do not allow all the turbulent scales to be modelled, then the filtered scales must be taken into account by semi-empirical models. It is possible to perform a low-resolution Navier-Stokes simulation, but significant empiricism must be introduced. For instance, if a Reynolds Averaged Navier Stokes (RANS) simulation is performed, the filtered scales are taken into account by the so called *turbulence model*, which is a non-universal formulation and its coefficients are achieved with experiments on simplified test cases.

For the high *Re* values of interest to naval architects, RANS is the most common solution. However, also RANS needs a significant computational effort compared to potential flow. During most of the 20$^{th}$ century the Navier-Stokes equations could be solved only for simple geometries and low *Re*, such as for blood flowing through arteries. At the end of the 20$^{th}$ century, the growth of computational resources allowed higher spatial and time resolutions to be achieved and higher *Re* to be modelled.

The correlation between the spatial resolution increase and the grown of the computational resources is well illustrated by the following example. In sail aerodynamics *Re* is one order of magnitude lower than in hull hydrodynamics due to the higher kinematic viscosity of the air. In upwind condition, the sails are trimmed near the maximum lift/drag ratio and the flow is mainly attached. Potential flow theory was effectively used since the 1970s [11, 12, 13] to model the flow around upwind sails. Conversely, in downwind conditions the sails are trimmed near the maximum lift and the flow field is characterised by leading edge separation, laminar-to-turbulent transition, reattachment, and trailing edge separation. Potential flow codes are unable to predict separation and cannot model the flow around downwind sails. The first RANS application on downwind sails was performed by Hedges in 1993 [14]. Since then, the continuous grown of the computational resources has led to increased spatial resolution. Figure 1 shows the velocity of the fastest computers in the world in gigaflops (left) and the number of cells (right) used in downwind sail aerodynamics from 1995 to 2008. The grow rate of both the computational resources and of the spatial resolution is about one order of magnitude every three years. After the first application by Hedges in 1993 [14], Miyata performed a milestone simulation in 1999 [15]. Then, during the 31$^{st}$ and the 32$^{nd}$ America's Cup, the top challengers used grids with a number of cells of the order of $10^5$ and $10^7$ respectively. In 2008, Viola [16] performed a milestone simulation of 37 millions elements and, in the same year, Viola & Ponzini [17] performed the largest grid ever done reaching a billion cells.

This example clearly shows that the spatial resolution used in RANS applications will certainly increase in the future together with the grown of the computational capability. The higher the number of cells of the grid, the higher is the spatial resolution and thus the less the simulation relies on the turbulence model, which is a non-universal semi-empirical formulation. The increase in the spatial and time resolutions will also allow different techniques for solving the Navier-Stokes equations to be efficiently used in the design process, such as Detached Eddy Simulation (DES) and Large Eddy Simulations (LES), which are too time consuming at the current state of the art.

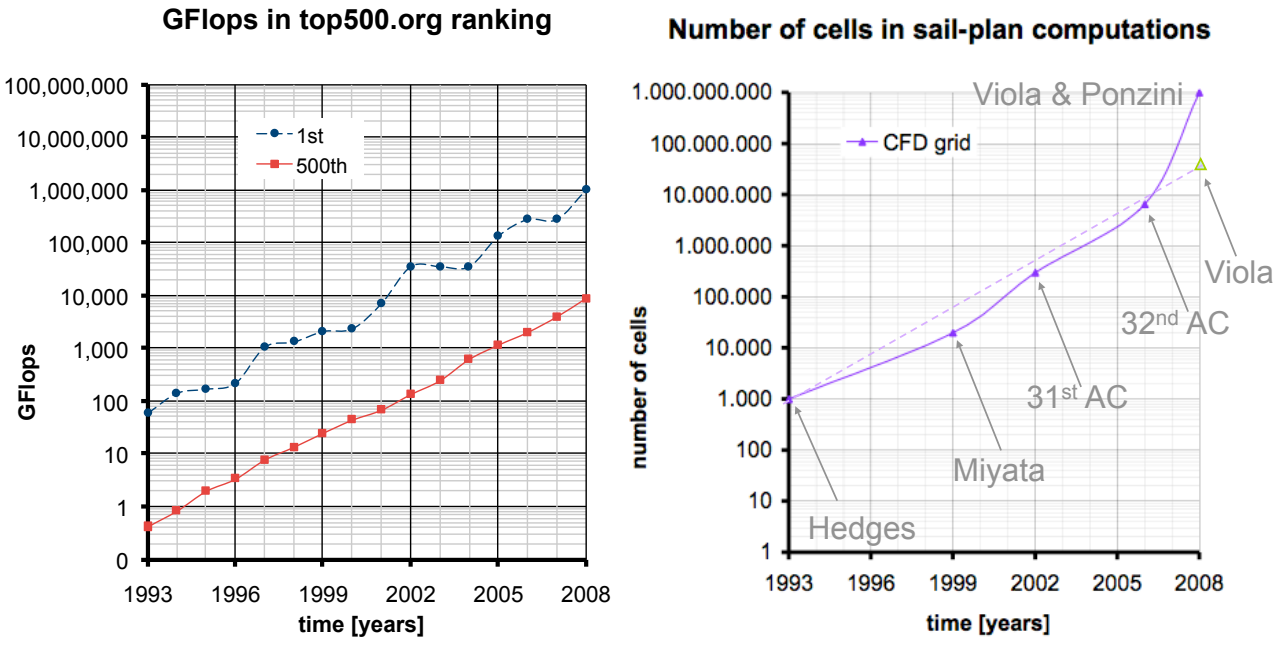


Figure 1: Maximum speed of the 1$^{st}$ and 500$^{th}$ fastest computers in the world (left) and number of cells used in RANS simulations for sail aerodynamics from 1993 to 2008.

## 2. RANS FEATURES AND LIMITATIONS

RANS codes were used since the 1980s for stern/wake flows but only in 1994 a significant number of codes modelling the free surface were presented in a conference: the Computational Fluid Dynamics (CFD) Workshop in Tokyo [18]. Most of these codes used the *interface tracking* techniques, which require the grid to follow the free surface and cannot model breaking waves. Later in the 1990s, more flexible *interface capturing* techniques with a *volume of fluid* approach [19] were widely implemented opening to a wider range of applications. In 1997 Orihara and Miyata [20] performed a free to sink and trim simulation of a semi planning boat, while Miyata et al. 1997 [21] performed a free to sink, trim and heel sailing yacht. In 2001 Azcueta [22] performed 6 degree of freedom (DOF) simulations.

RANS simulations in the marine fields have become much more widely used during the last decade. The state of the art is well presented by the *CFD Workshop Tokyo 2005* [23] and the *Gothenburg 2010*: *A Workshop on CFD in Ship Hydrodynamics* [24], where the impact of RANS in ship hydrodynamics was discussed. It was noted that it is successfully extending to the prediction of 6 DOF ship motions for seakeeping and maneuverability. However, the RANS capability of accurately modelling large amplitude ship motions like stall and the interactions between hull and appendages was discussed.

CFD users are increasingly aware of the need of verification and validation (V&V) procedures, in particular for unsteady forces in time domain. Conversely, V&V has been often ignored in the yacht and super yacht field. In the opinion of the author, while a significant effort has been spent on exploring the modelling capabilities of RANS, not enough effort has been spent on verifying the simulation and validating the model. Moreover, validation has been often misleading by the lack of verification. Incorrect results have led to scepticism about RANS capabilities. Conversely, the authors are enthusiastic about it, as long as the uncertainty of the solution is always carefully explored and taken into account by the designer.

### 2.1 VERIFICATION AND VALIDATION

As explained above, RANS requires the turbulence model to estimate the effect of the spatial and temporal filtered fluctuations on the averaged velocity and pressure fields. Therefore, the solution does necessarily depend upon both the spatial and time discretization, and on the turbulence model. A numerical solution also depends on the algorithms used to estimate the solution at the successive iteration. Moreover a converging iteration process tends towards a solution, but a finite number of iterations led necessary to a difference between it and the actual solution. Finally, the geometry and the conditions modelled numerically are inevitably slightly different from the real geometry, which is usually more detailed, and also the real conditions, which usually have more dynamics than which is modelled. Therefore there are many sources of errors and the uncertainty of the solution must be evaluated. It should be noted that also potential flow codes and experimental techniques have various sources of errors and the uncertainty must be equally considered.

The validation and verification (V&V) process was initiated by Roache in 1994 [25] with the grid converge index to estimate the uncertainty due to the spatial and temporal discretization. The V&V process was also developed by the American Institute of Aeronautics and Astronautics (AIAA) Committee on Standards for CFD [26, 27] and by the American Society of Mechanical Engineers (ASME) in 2009 [28, 29]. The ITTC also provided guidelines in 2002 [30] and updated guidelines are expected soon.

The difference between the computed value $S$ and the true value $T$ is the simulation error $E$. This is due to the numerical error $\delta_{SN}$ - which includes errors due to the iteration number $\delta_i$, grid size $\delta_g$, time step $\delta_t$, and other input parameters $\delta_p$ - and to the numerical modelling $\delta_{SM}$.

$$E = S - T = \\ = \delta_{SN} + \delta_{SM} = (\delta_i + \delta_g + \delta_t + \delta_p) + \delta_{SM} \qquad (1)$$

The verification process assesses the numerical uncertainty $U_{SN}$ at 95% confidence level due to the numerical error $\delta_{SN}$. In particular, it assesses the uncertainty components due to the iteration number $U_i$, grid size $U_g$, time step $U_t$, and other input parameters $U_p$.

The validation process assesses the modelling uncertainty $U_{SM}$ due to the modelling error $\delta_{SM}$. The overall simulation uncertainty is estimated as per experimental fluid dynamics uncertainty analysis:

$$U_S^2 = U_{SN}^2 + U_{SM}^2 = (U_i^2 + U_g^2 + U_t^2 + U_p^2) + U_{SM}^2 \qquad (2)$$

The numerical uncertainty $U_{SN}$ is estimated performing several simulations and evaluating the trend of the results. The largest uncertainties are due to the grid size $U_g$ and time step $U_t$. These uncertainties are evaluated performing several simulations with different grid sizes and time steps respectively. Increasing the spatial and time resolutions, the solution should converge (monotonically or oscillating) to a grid-size and time step, respectively, independent solution. Too coarse grids and too large time steps lead to non-converging trends and unreliable solutions. If a convergent trend is achieved, $U_g$ and $U_t$ are estimated on the basis of the order of convergence. The convergence analysis allows also extrapolating the numerical solution S to an infinitely high spatial and time resolutions (*Richardson Extrapolation*).

The validation is performed comparing the numerical solution S with the experimental results D. The uncertainty of the validation $U_{val}$ is due to the numerical uncertainty $U_{SN}$ and to the experimental uncertainty $U_D$:

$$U_{val}^2 = U_{SN}^2 + U_D^2 \quad (3)$$

The simulation is validated if the absolute value of the error $E = S - D$ is smaller than the validation uncertainty $U_{val}$. In fact, the validation uncertainty is a measure of the 'noise' in the comparison between the numerical and experimental data. If the error is lower than the noise - and the simulation is validated - than no conclusions can be drawn about the modelling error. Conversely, if the error is larger than the noise - and the simulation is not validated – than the error is (partially) due to modelling error.

For a design prospective, solution from both validated and non-validated simulations can be used. In fact, if the modelling error is estimated, it could be sufficiently small to be neglected for design purpose. While the designer is often interested in the amplitude of the numerical error, they often underestimate the importance of the verification process, i.e. of the numerical uncertainty. It is the opinion of the authors that a numerical simulation should always be presented with the results of the verification process.

## 2.2 EXAMPLE OF VERIFICATION AND VALIDATION

An example is presented to clarify this concept. A 105 foot motor yacht (Figure 2) was modelled with the finite-volume code STAR-CCM+ (CD-adapco). The hull was designed by Hydro Tec and the launch is due by 2012.
A domain 4L x 1.8L x 1.5L in length, height and depth was discretized with about 600,000 hexahedral cells. Zero yaw and heel was considered and thus only half of the yacht was modelled taking advantage of the yacht symmetry. The cells were oriented with the Cartesian axis and trimmed by the boat surface [28]. A RANS simulation was performed using the $k-\epsilon$ *relizable* model and *two-layer all-y+* [31] wall function. The averaged y+ value was about 80 along the hull. The Volume Of Fluid (VOF) approach was used to model the two phases and a High Resolution Interface Capturing (HRIC) interpolation scheme was used to model the free-surface. A constant velocity $V$ was used at the inlet with 1% turbulence intensity and turbulent/physical viscosity ratio of 10. The simulations were performed both in model scale and in full scale, and the results were compared with towing tank tests. The model was both physically tested and numerically modelled in free to sink and trim condition. The grid was rigidly moved with respect to the boundary conditions in order to take into account the sink and trim movements. Time steps of 0.02s were used and 200s were modelled in order to achieve a steady result.

Figure 2: Rendering of the 105 foot motor yacht tested

Figure 3 shows the numerical ('*NUM*') and the experimental ('*EXP*') resistance coefficient $C_T$ at model scale versus *Fr*, where:

$$C_T = \frac{R}{\frac{1}{2}\rho V^2 A_W} \quad (4)$$

$R$ is the resistance, $\rho$ is the density of the water, $A_W$ is the wetted surface.

Figures 4 shows the numerical and the experimental trim at model scale.

The model-scale experimental results were corrected with the ITTC'57 model-ship correlation line in order to achieve the full-scale resistance. Table 1 shows the corrected experimental resistance coefficient and the numerical resistance computed at full-scale. The comparison is performed at the design speed ($Fr = 0.395$).

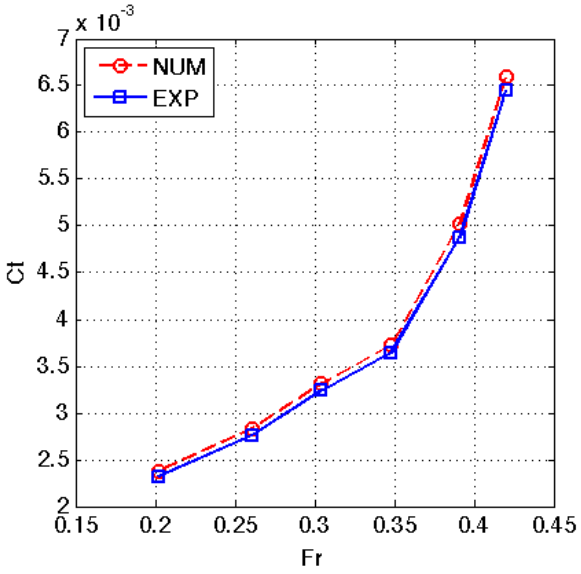


Figure 3: Numerical and experimental $C_T$ at model scale.

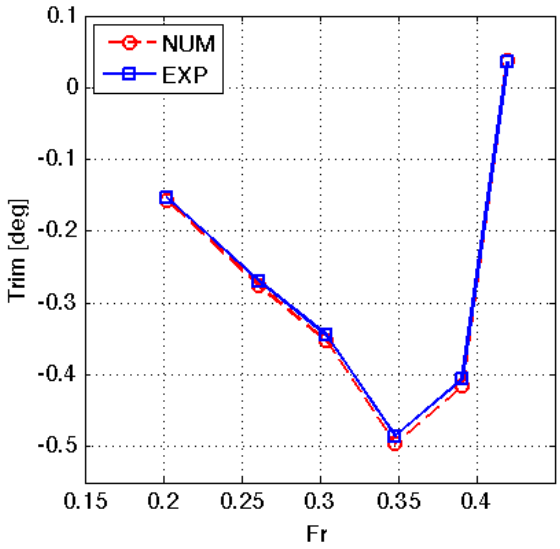

Figure 4: Numerical and experimental trim at model scale.

Table 1: Full-scale $C_T$ at $Fr = 0.395$.

| | |
|---|---|
| $C_{T\,EXP}$ | $9.684 \cdot 10^{-3}$ |
| $C_{T\,NUM}$ | $9.815 \cdot 10^{-3}$ |
| $(C_{T\,NUM} - C_{T\,EXP}) / C_{T\,EXP}$ | + 1.33% |

The numerical and experimental results are in very good agreement both in model scale and in full scale. The maximum numerical-experimental difference is about 3.1% and 1.3% in model scale and full scale respectively for the resistance, while the maximum differences in the trim is 0.01 degrees in model scale.

It is interesting to note that the trim increases of about 0.1 degree at $Fr = 0.395$ when the simulation is performed in full scale instead of model scale.

A verification analysis of the full-scale simulation was performed. The grid size and the time step used in the simulations were used as reference values. One finer grid and two coarser grids were tested. Several time steps were also investigated. In particular, the time step was divided by $\sqrt{2}$ and 2, and multiplied by $\sqrt{2}$.

Figures 5-8 show the computed $C_T$ and trim, divided by the values achieved with the base grid size and base time step, versus the *relative step sizes*. In Figure 5-6, the relative step size is the actual number of cells divided by the one used in the base grid. Similarly, in Figure 7-8, the relative step size is the time step divided by the base one. Uncertainty bars at 95% confidence level are showed. The uncertainty and the orders $p$ of the regression curves were computed following the guidelines in [32]. Figure 6 shows that an infinitely fine grid would lead to a $C_T$ 10% lower than what was used in the base simulation. Therefore, the numerical/experimental comparison showing an absolute error of 1.33% (Table 1) performed without a verification analysis is misleading.

The uncertainties due to the iteration number, grid size, time step, and other input parameters should be summed to compute the numerical uncertainty. It is often assumed that the uncertainties due to the grid size and time step are much larger than the uncertainty due to the iterations and others inputs, the numerical uncertainties are:

$$U_{SN} = \sqrt[2]{U_g^2 + U_t^2} \tag{5}$$

In this example, the numerical uncertainty of the resistance due to the time step is negligible and thus the numerical uncertainty is equal to the uncertainty due to the grid size only. The grid refinement (Figure 5) shows that the resistance coefficient used in Table 1 is computed with an uncertainty of 12% with 95% confidence. In order to decrease the uncertainty, a finer grid should be used. For instance, if the finest grid showed in Figure 1 were used, the uncertainty would have dropped to 10%. If very high accuracy is required, then a grid refinement should be performed at every speed and the extrapolated value could be used. For instance, figure 6 shows that if the extrapolated value were used, the uncertainty would be only 2%. Assuming an oscillating convergence (Figure 6), the trim is computed with higher spatial resolution than the resistance. For the base simulation, the uncertainties are about 1.3% and 2.2% because of the grid size and time step respectively, leading to a numerical uncertainty (5) of 2.3%.

The extrapolated resistance is computed with an uncertainty (5) of $U_{SN} = 2\%$. Considering an experimental uncertainty of about 2.5% (as for instance in [24]), the validation uncertainty (3) is $U_{val} = 3.2\%$. The error between the extrapolated resistance and the experimental data is $E = -8\%$. Therefore the simulation is not validated because $|E| > U_{val}$, which shows that there is a modelling error $\delta_{SM}$, probably due to the model-ship correlation adopted to scale the experimental viscous resistance. However, the large grid uncertainty for the finest grid (Figure 5) and the low order of convergence suggest that higher spatial resolution should be used.

A V&V analysis performed on the model-scale simulations is also necessary and the validation procedure would allow verifying if the modelling error is due to an incorrect numerical setup. This example shows that a numerical-experimental comparison performed without a verification procedure, can hide a significant modelling error. Moreover, it should be noted that the uncertainties of the non-extrapolated results can be very high.

In conclusion, a numerical/experimental comparison performed without a rigorous V&V procedure should be considered with great caution. It is quite common that a bias due to a modelling error leads to the under-estimation of the fluid dynamic forces. On the other

hand, coarse grid used to model the boundary layer and low-order discretization schemes can lead to force over-overestimation. When these occur simultaneously, very good numerical/experimental comparison might occur hiding major errors in the simulation.

The results showed in Section 2 show that RANS analysis can provide very useful information but its uncertainty should always be considered. The most complicated the modelled physics, the highest the uncertainty. In free to sink and trim condition and flat water, an uncertainty below 5% should be achieved. Conversely, when a yacht is modelled with 6DOF sailing in rough see, a very large uncertainty should be expected. Therefore, when a simulation is planned, it is very important to choose between the opportunity of performing more complicated simulations leading to higher uncertainties, and performing simpler simulations with lower uncertainty. Moreover if the experimental data is not available, the validation cannot be performed and the modelling error cannot be estimated.

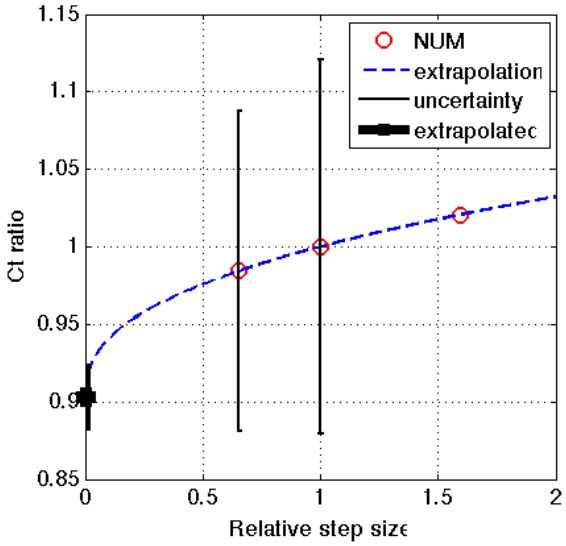

Figure 5: Resistance variations vs spatial resolution

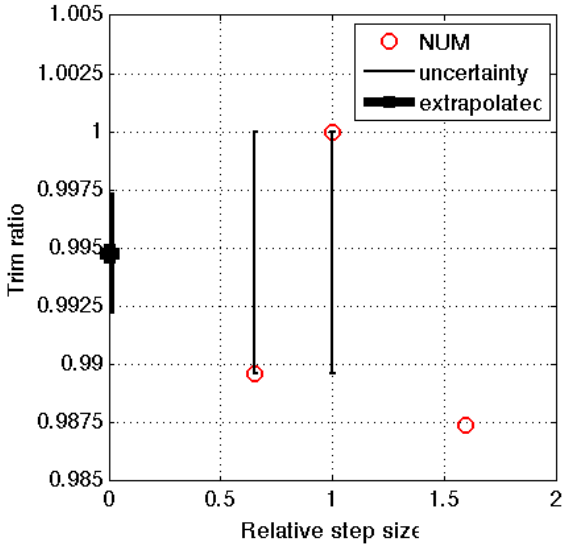

Figure 6: Trim variations vs spatial resolution

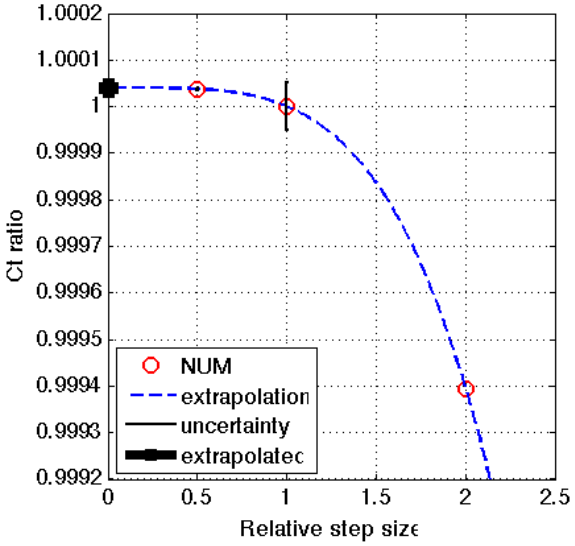

Figure 7: Resistance variations vs time resolution

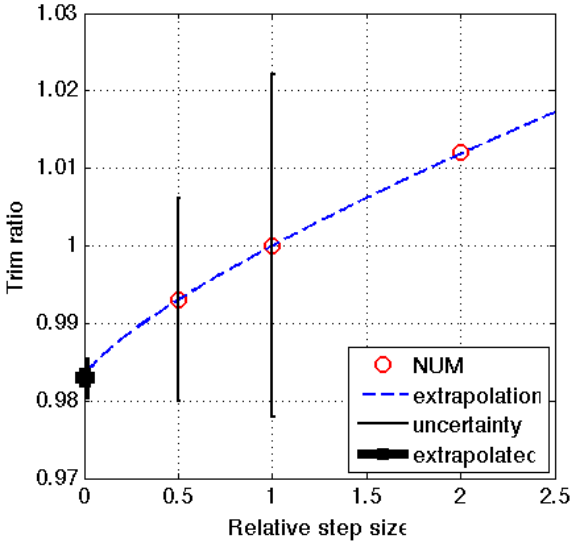

Figure 8: Trim variations vs time resolution

## 3. CHOOSING A METHOD: EXPERIMENTS, POTENTIAL FLOW OR RANS

In this section, examples of applications are given with the aim of showing that the usage of experimental methods, potential flow codes and RANS codes can provide substantial benefits if used according to their features and limitations.

### 3.1 HULL RESISTANCE

In the early stage of the design process, potential flow codes can provide valuable information about the wave resistance. In particular, the effect of hull form factors on the wave resistance can be investigated. The main advantage of potential flow codes is the low run time required. Moreover, they can be coupled with optimisation codes in order to investigate multi-objective functions [33]. However, in most of the cases the

optimum design cannot be found with these codes due to their inability of modelling viscous effects, and thus friction resistance and separated flow. For instance, the design with the lowest wave resistance might have a higher resistance due to separation or larger wetted surface.

In an advanced design stage, RANS codes should be used. As shown in the previous sections, the simulation might present large numerical and modelling error. Therefore, V&V are required. In order to estimate the modelling error, the experimental data is necessary. A representative design could be experimentally tested in all the conditions that have to be numerically modelled. For instance, a motor yacht can be tested at several speeds in upright condition without leeway, while a sailing yacht can be tested in several heeling and yaw conditions as well for at least one speed. The experimental uncertainly should be estimated. Validation can then be performed on the experimentally tested design; assuming that the modelling error would not change significantly when different design candidates are modelled. When two design candidates are compared, conclusions should be drawn only if the simulations are validated and if the numerical uncertainty is lower than the differences between the results for the two candidates.

One of the advantages of comparing several design candidates with RANS codes instead of with only experimental tests is that the numerical results can be more easily integrated into the design spiral. In fact, when the V&V have been performed, the resistance curve of an additional design candidate can be performed in few hours. Conversely, in order to test a new candidate in the tank several weeks are necessary to make the model, perform the test and receive the report. In this approach, the experimental test is performed with the aim of validating the numerical results. The numerical simulation should thus model the experimental test, at the *Fr* and *Re* used in the towing tank. The towing tank uncertainty must be known and should be taken into account. If the numerical simulation models the full-scale condition, then the validation cannot be properly performed because the uncertainty of the methods to correct the experimental friction resistance is unknown.

## 3.2 HULL APPENDAGES

Appendages can be investigated with several methods. Ventilation and cavitation can be adequately investigated with experimental tests. In particular, cavitation cannot be modelled with potential flow codes and it is modelled with difficulties with RANS codes. During the conclusive general discussion at the *Developments in Marine CFD* conference, London March 22nd - 23rd, 2011, it was agreed that about 50 million cells per blade are necessary to accurately model the cavitation on propellers.

The design of keels and rudders can be effectively investigated with numerical methods. Both potential flow codes and RANS codes must take into account the laminar-to-turbulent transition in order to correctly predict the resistance. For instance, the potential flow code XFOIL allows computing both forced and free transition, and transitional separation bubbles.

The geometry and the position of fin stabilizers are investigated with difficulty with potential flow codes and experimental methods. In fact, fin stabilizer is an airfoil with low aspect ratio and thus the viscous effects at the tip are significant. Della Rosa et al. [34] showed that potential flow codes increasingly under-predict the drag when the angle of attack increases. However, potential flow codes might be used for a preliminary investigation of the two-dimensional section of the fin. Experimental tests might be difficult because the drag of the fin stabilizer is significantly lower than the drag of the entire hull. The investigation of the position of the fin involves the study of the streamline along the hull, which could be done both with RANS codes and experimentally.

As an example, the author designed a two-dimensional section of a fin stabilizer using the potential flow code XFOIL coupled with a genetic algorithm based code [34]. The design objectives were the maximum lift/drag ratio at 3 degree angle of attack, and the maximum lift. The optimum section was then used to design the three-dimensional fin, which was modelled with STAR-CCM+ (CD-adapco). The analysis of the fin in isolation allowed the design of the endplate, sweep angles and taper ratio to be enhanced.

The zero-speed condition was also modelled. When the yacht is at anchor, the fin can rotate of about 60 degree in 10 seconds leading to a significant roll moment, which can be used to counteract the roll moment due to waves.

Additional analysis was performed in order to investigate the best fin/hull configuration. The hull was the 105 foot power yacht presented in §2.2. Two possible configurations were considered: one fin per side and two fins per side (Figure 9).

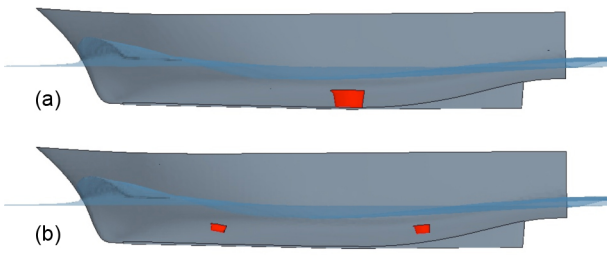


Figure 9: Fin's position and geometrical alignment. (a) one fin per side; (b) two fins per side.

The fins used in the two configurations were geometrically similar but were scaled in order to keep the same wetted surface and not to increase the maximum

draft and beam of the hull. A multiphase RANS analysis performed with a similar setup than the one described in §2.2 allowed the streamlines along the hull to be computed at several yacht speeds considering the free-surface effect, and thus to align the fins in order to avoid wake interference. The difference in the resistance computed for the two configurations was of the order of 1% and lower than the simulation uncertainty.

### 3.3 PROPELLERS

From a design point of view, RANS investigations of propellers and cavitation are too computational expensive. RANS and potential flow codes can be used together efficiently if the flow around the hull is modelled with a RANS code and the flow at the propeller disk is transferred to the potential flow code which model the propeller. For instance, Villa et al [35] developed a coupled method where the RANS solution at the disk is transferred to the potential flow coded as equivalent body forces.

Cavitation can be explored very efficiently with model-scale tests in cavitation tunnels. For instance, the Emerson Cavitation Tunnel at the Newcastle University has a test section 3.10 x 1.22 x 0.81 m and can test different kind of propulsors up to 0.4 m in diameter. The maximum velocity of 10 m/s and pressures from 7.6 to 106 kN/m$^2$ which allows reach on cavitation numbers from 0.5 to 2.

The authors performed a RANS investigation of a 163 foot motor yacht with two propeller shafts using the code Fluent (Ansys Inc.). In order to save computational time without compromising the spatial resolution, a multi-phase simulation of the yacht without the propeller shafts was performed in a free to sink and trim condition. Then a subdomain near the propeller shafts was identified. The solution of the multi-phase simulation was used to set the boundary conditions of the mono-phase simulation modelling the subdomain with the propeller shafts (Figure 10), taking into account the trimmed and surged position of the hull, and the disturbed free surface. A steady RANS simulation using the $k-\omega$ *SST* turbulence model were performed. In particular, only half body was modelled using the symmetry plane of the yacht and a tetrahedral grid of about 2.3 million cells was made with Gambit and Tgrid (Ansys Inc.). The grid was refined in order to achieve y+ of the order of 60 both along the hull and on the appendages. The effect of the accentuated longitudinal curvature of the hull in correspondence of the propeller disks on the velocity and pressure fields was investigated. Figure 11 shows the dynamic pressure (divided by the inlet dynamic pressure) on the longitudinal plane of a propeller shaft. The velocity and pressure fields at the propeller disk were then used by the Department of Naval Engineering, Universita' degli Studi di Genova, as input for the potential flow code modelling of the propeller.

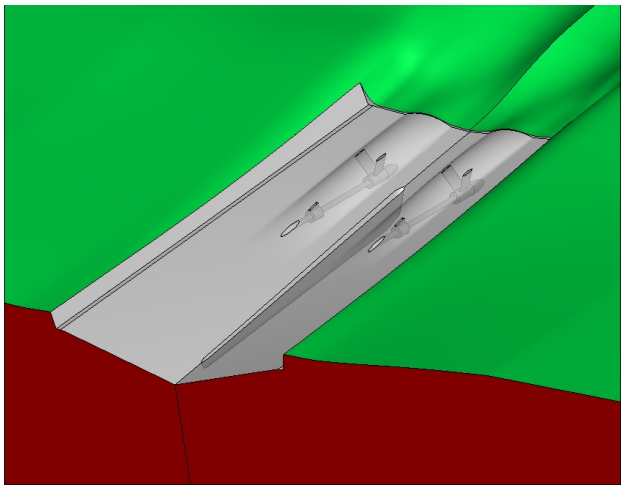

Figure 10: Subdomain near the propeller shafts.

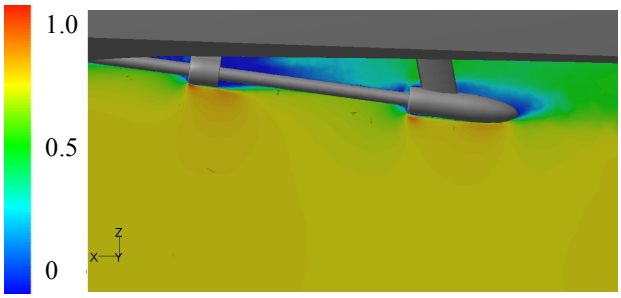


Figure 11: non-dimensional dynamic pressure on the longitudinal plane.

## 4. CONCLUSIONS

The paper discusses the features and the limitations of full-scale and model-scale experimental tests, potential flow and Navier-Stokes codes, with the emphasis on RANS codes.

RANS codes are particularly computational demanding and therefore their usage increased with the grown of computational resources. In the recent years, the capabilities of RANS codes have been thoroughly investigated while the associated uncertainty of the numerical results have been often underestimated. In fact, RANS codes can model a very wide range of complex physics, but the spatial and time resolutions required to achieve small uncertainty in the result can be extremely high. In general, the higher the complexity of the simulation, the higher the uncertainty of the result. Similar considerations can be applied to potential flow codes. However there is more awareness of the potential flow code limitations than the RANS code limitations.

The main advantage of RANS codes is their capability of modelling viscous phenomena, which potential flow codes cannot do. Moreover, RANS codes provide the velocity and pressure fields in the entire computational volume while potential flow codes provide the velocity

and pressure fields on three-dimensional surfaces. The main draw back is the longer run time and the higher expertise required to correctly setup the simulation.

Experimental tests are fundamental to perform the validation of the numerical codes. Moreover, in some applications the experimental uncertainty can be very low and the same uncertainty can be achieved with difficulties with numerical methods. For instance, cavitation can be tested in cavitation tunnel and very accurate measurements can be performed, while RANS codes require a very high spatial and time resolutions in order to achieve the same uncertainty.

Each of the three methods has their own unique features and they must be used with a thorough understanding of their limitations, so as to provide a reliable suite of design tools.

## 5. ACKNOWLEDGMENTS

The support of CD-adapco, Ansys Inc. and CNC Marine is gratefully acknowledged. The authors are also very grateful to Richard Carter for his very generous and precious help.

## 6. REFERENCES

1. Froude, W., Report to the Lords Commissioners of the Admiralty on experiments for the determination of the friction resistance of water on a surface, under various conditions, performed at Chelson Cross, under the authority of Their Lordships, *44th Report of the British Association for the Advancements of Science, 249-255,* 1874.

2. Prandtl, L., Bericht über Untersuchungen zur ausgebildeten Turbulenz, *Z. Angew, Math, Meth., vol 5, pp 136-139,* 1925.

3. von Kármán, T., Über laminare und turbulente Reibung, *Z. Angew. Math. Mech., vol 1, pp 233-252,* 1925 *(English translation in NACA Technical Memo. 1092).*

4. Blasius, H., Grenzschichten in Flüssikeiten mit kleiner Reibung, *Z. Angew. Math. Phys., vol 56, pp 1-37,* 1908 *(English translation in NACA Technical Memo. 1256).*

5. Hughes, G., Frictional resistance of smooth plane surfaces in turbulent flow, *Trans. Inst. Naval Archit. 94,* 1952.

6. Hughes, G., Friction and form resistance in turbulent flow and a proposed formulation for use in model and ship correlation, *Trans. Inst. Naval Archit. 96,* 1954.

7. International Towing Tank Conference, Proceedings of the 8th ITTC, Madrid*, Canal de Experiencias Hidrodinamicas, El Pardo, Madrid, Spain,* 1957.

8. Navier, C.L.M.H., Mémoire sur les lois du mouvement des fluides, *Mem. Acad. R. Sci. Paris*, vol *6, pp 389-416,* 1823.

9. Stokes, G.G., On the theories of the internal friction of fluids in motion, and of the equilibrium and motion of elastic solids, *Trans. Camb. Phil. Soc., 8, 287–305,* 1845

10. Spalart, P.R., Direct simulation of a turbulent boundary layer up to Reθ = 1400, *J. Fluid Mech., 187, 61-98,* 1988.

11. Milgram, J.H., The Aerodynamics of Sails, *Proc of the 7th Symposium of Naval Hydrodynamics*, *unsteady propeller forces, fundamental hydrodynamics, unconventional propulsion ; August 25 – 30 ,1968 Rome, Italy. Ralph D Cooper & Stanley W Doroff (eds). Arlington, Va. : Office of Naval Research, pp. 1397-1434,* 1968.

12. Milgram, J.H., The Analytical Design of Yacht Sails, *SNAME Annual Meeting / Trans SNAME*, vol *68, pp. 118-160,* 1968.

13. Gentry, A.E., The Aerodynamics of Sail Interaction, *Proc. of the 3rd AIAA Symp on the Aero/Hydronautics of Sailing, Redondo Beach, CA, USA, 20 Nov 1971.*

14. Hedges, K.L., Computer Modeling of Downwind Sails, *New Zealand, University of Auckland, ME Thesis, 85 pp,* 1993.

15. Miyata, H., Lee, Y.W., Application of CFD Simulation to the Design of Sails, *J. Marine Science & Tech, Vol. 4, pp. 163-172,* 1999.

16. Viola, I.M., Downwind Sail Aerodynamics: a CFD Investigation with High Grid Resolution, *Ocean Eng, vol. 36, issues 12-13, pp. 974-984,* 2009.

17. Viola, I.M., Ponzini, R., A CFD Investigation with High-Resolution Grids of Downwind Sail Aerodynamics, *RINA Intl. Conf. on Developments in Marine CFD,; 22-23 Mar 2011, London, UK, RINA, pp 99-110,* 2011.

18. Kodama, Y., Takeshi, H., Hinatsu, M., Hino, T., Uto, S., Hirata, N., Murashige, S. (editors), *Proc. of CFD Workshop Tokyo 1994: An Intl. Workshop for Improvement of Hull Form Designs, 22-24 March 1994, Tokyo, Japan. Japan, Ship Res. Inst., 2 vols,* 1994.

19. Larsson, L., Regnstrom, B., Broberg, L., Li D-Q., Janson, C-E, Failures, Fantasies and Feats in the Theoretical/Numerical Prediction of Ship Performances, *Proc. of the 22nd Symp. on Naval Hydrodynamics*, *Washington, DC, Aug 1998. USA, NAP, pp 11-32.* 1998.

20. Orihara, H., Miyata, H., CFD Simulation of a Semi-planing Boat in Unsteady Motion, *FAST '97, 4th*

*International Conf. on Fast Sea Transportation, Jul 1997, Sydney, Australia. Baird Publications, vol 1, pp 35-42,* 1997.

21. Miyata, H., Akimoto, H., Hiroshima, F., CFD Performance Prediction Simulation for Hull-form Design of Sailing Boats, *J. Marine Science & Tech., vol 2, pp 257-267,* 1997.

22. Azcueta, R.R., Computational of Turbulent Free-surface Flows Around Ships and Floating Bodies, Technishen Universitat Hamburg-Harburg, Doktor-Ingenieur genehmigte Disseratation (PhD thesis), 105 pp, 2001.

23. Hino, T. (editor), *The Proc. of the CFD Workshop Tokyo 2005, Tokyo, Japan, 9–11 March* 2005. *Japan, National Maritime Res. Inst,* 2005.

24. Larsson, L., Stern, F., Bertram, V., Benchmarking of Computational Fluid Dynamics for Ship Flows: the Gothenburg 2000 Workshop, *J. Ship Res, vol 47, no 1, pp 63–81,* March 2003. & www.Gothenburg2010.org (revised edition of 2003 paper in press)

25. Roache, P., Perspective: a Method for Uniform Reporting of Grid Refinement Studies, *ASME J. Fluids Eng, vol 116, pp 405-413,* Sept 1994.

26. Rahaim, C.P., Oberkampf, W.L., Cosner, R.R., Dominik, D.F. AIAA Committee on Standards for CFD-Status and Plans, *41st Aerospace Sciences Mtg, Reno, Nevada, 6–9 Jan 2003. USA; Paper AIAA-2003-844,* 2003.

27. AIAA. Guide for the Verification and Validation of Computational Fluid Dynamics Simulations, *USA; Guide AIAA-G-077-1998, 19 pp,* 1998.

28. ASME. Standard for Verification and Validation in Computational Fluid Dynamics and Heat Transfer, *USA; ASME, VV20-2009, 88 pp,* 2009.

29. Freitas, C.J., Ghia, U., Celik, I., Roache, P., Raad, P., ASME's Quest to quantify numerical uncertainty. *41st Aerospace Sciences Mtg, Reno, Nevada, 6–9 Jan 2003. USA; Paper AIAA-2003-627,* 2003.

30. ITTC, The Resistance Committee., Uncertainty Analysis in CFD, Verification and Validation Methodology and Procedures, *23rd Intl. Towing Tank Conf.; 8-14 Sept 2002, Venice, Italy., ITTC-Quality Manual, CFD General, 7.5-03-01-01,* 2002.
www.ittc.sname.org/2002_recomm_proc/7.3-03-01-01.pdf

31. CD-adapco, *User Guide STAR-CCM+ Version 4.06.011,* 2009.

32. Stern, F., Wilson, R., Shao, J., Quantitative V&V of CFD Simulations and Certification of CFD codes, *Intl. J. Numerical Methods In Fluids, vol 50, no 11, pp 1335-1355,* 20 April 2006.

33. Rosenthal, B., Multi-objective Optimization of a High-speed Vessel with Integrated Bow Lifting Body, *RINA Intl. Conf. on Developments in Marine CFD,; 22-23 Mar 2011, London, UK, RINA, pp 153-160,* 2011.

34. Della Rosa, S., Maceri, M., Viola, I.M., Bartesaghi, S., Design and Optimization of a Fin Stabilizer Using CFD Codes and Optimization Algorithms, *Nav 2009. Proc. 16th Intl. Conf. of Ship & Shipping Research, 26-27 Nov 2009, Messina, Italy. Italy, ATENA,* 2009.

35. Villa, D., Gaggero, S., Brizzolara, S., Simulation of Ship in Self-Propulsion with Different CFD Methods: From Actuator Disk to Potential Flow coupled solvers to fully unsteady RANS model, *RINA Intl. Conf. on Developments in Marine CFD,; 22-23 Mar 2011, London, UK, RINA, pp 1-12,* 2011.

## 7. BIOGRAPHIES

**Ignazio Maria Viola** holds the current position of Lecturer in Naval Architecture at the School of Marine Science and Technology of the Newcastle University in UK. Ignazio's specialist skills and experience are in numerical and experimental fluid dynamics. His main research focus is high-performance sailing yachts and, in particular, sail aerodynamics and hull hydrodynamics. He is member of the Yacht Research Unit at the University of Auckland where he performed a Post Doctoral Fellow collaborating with the America's Cup challenger Emirates Team New Zealand. He was awarded a PhD at the Politecnico di Milano Wind Tunnel, (funded by the Luna Rossa Challenge for the 32nd America's Cup) for a thesis on the numerical and the experimental analysis of America's Cup sail plans. His research portfolio also includes the aerodynamics of trains, cars, long- span bridges and tall buildings.

**Simone Bartesaghi** is PhD student at the Mechanical Department of the Politecnico di Milano, where he is responsible for KB/Embedded CFD Simulations. He was awarded a master degree in Mechanical Engineering at the Politecnico di Milano with a thesis on methods and techniques of virtual prototyping. He was also awarded a master in Yacht Design (marks 110/110) at the Politecnico di Milano and Università degli Studi di Genova. Before the PhD, in collaboration with Porto Ricerca snc, he performed the RANS simulations for the VOR70-class yacht of CAMPER/ETNZ, challenger of the Volvo Ocean Race 2011-2012.

**Silverio Della Rosa**, aerospace engineer founder and Director of Silverio Della Rosa Naval Architect, provides fluid dynamics and structural engineering consultancy for the marine and wind energy industries. His previous experience includes the design of Nytec yachts, the 555FIV dinghy, and the tank testing for *Italia*, challenger of the America's Cup in 1987.

**Sergio Cutolo** is Hydro Tec's soul and mind. He founded the company in 1995 after a vibrant career with some of the leading shipyards of the world. His career was kicked off with a Naval Engineering degree from the "Federico II" university in Naples, Italy.